Mon. Not. R. Astron. Soc. **000**, 000–000 (0000) Printed 30 October 2014 (MN LATEX style file v2.2)

Kelvin-Helmholtz Instability of Counter-Rotating Discs

Dan Quach[1], Sergei Dyda[1], and Richard V. E. Lovelace[2]
[1]*Department of Physics, Cornell University, Ithaca, NY 14853, USA*
[2]*Department of Astronomy, Cornell University, Ithaca, NY 14853, USA*

30 October 2014

arXiv:1408.5625v2 [astro-ph.GA] 29 Oct 2014

ABSTRACT

Observations of galaxies and models of accreting systems point to the occurrence of counter-rotating discs where the inner part of the disc ($r < r_0$) is co-rotating and the outer part is counter-rotating. This work analyzes the linear stability of radially separated co- and counter-rotating thin discs. The strong instability found is the supersonic Kelvin-Helmholtz instability. The growth rates are of the order of or larger than the angular rotation rate at the interface. The instability is absent if there is no vertical dependence of the perturbation. That is, the instability is essentially three-dimensional. The nonlinear evolution of the instability is predicted to lead to a mixing of the two components, strong heating of the mixed gas, and vertical expansion of the gas, and annihilation of the angular momenta of the two components. As a result the heated gas will free-fall towards the disc's center over the surface of the inner disc.

Key words: accretion, accretion discs, counter-rotating discs

1 INTRODUCTION

Commonly considered models of accretion discs have gas rotating in one direction with a turbulent viscosity acting to transport angular momentum outward and matter inward. However, observations indicate that there are more complicated, possibly transient, disc structures on a galactic scale. Observations of normal galaxies have revealed co/counter-rotating gas/gas, gas/stars, and stars/stars discs in many galaxies of all morphological types — ellipticals, spirals, and irregulars (Rubin 1994a, 1994b; Galletta 1996; recent review by Corsini 2014). There is limited evidence of counter-rotating gas components in discs around stars (Remijan and Hollis 2006; Tang et al. 2012). Theory and simulations of co/counter-rotating gas/gas discs around stars and black holes predict enormously enhanced accretion rates resulting from the presence of the two components which can give rise to outbursts from these discs (Lovelace and Chou 1996; Kuznetsov et al. 1999; Nixon, King, and Price 2012; Dyda et al. 2014).

Counter-rotation in disc galaxies appears in a variety of configurations including cases where (1) two cospatial populations of stars rotate in opposite directions, (2) the stars rotate in one direction and the gas rotates in the opposite direction, and (3) two spatially separated gas discs rotate in opposite directions (Corsini 2014). Of particular interest here is the example of case (3), the "Evil Eye" galaxy NGC 4826 in which the direction of rotation of the gas reverses going from the inner (180 km s^{-1}) to the outer disc (-200 km s^{-1}) with an inward radial accretion speed of more than 100 km s^{-1}in the transition zone, whereas the stars at all radii rotate in the same direction as the gas in the inner disc, which has a radius of $\sim$ 1200 pc (Braun et al. 1994; Rubin 1994b).

On a stellar mass scale, Remijan and Hollis (2006) and Tang et al. (2012) found evidence of accretion of counter-rotating gas in star forming systems. Accreted counter-rotating matter may encounter an existing co-rotating disc as in low-mass X-ray binary sources where the accreting, magnetized rotating neutron stars are observed to jump between states where they spin-up and those where they spin-down. Nelson et al. (1997) and Chakrabarty et al. (1997) have proposed that the change from spin-up to spin-down results from a reversal of the angular momentum of the wind-supplied accreting matter. The interface between the oppositely rotating components would be subject to the Kelvin-Helmholtz instability.

In the formation of massive black holes in the nuclei of active galaxies, King and Pringle (2006, 2007) argue that in order for the rapid growth of the massive black holes (observed at high red-shifts) to be compatible with the Eddington limit on their emission, the gas accretion is from a sequence of clouds with randomly oriented angular momenta. This process would lead to the formation of a disc with the rotation direction alternating as a function of radius.

Section 2 develops the theory for the stability analysis and obtains explicit growth rates for the supersonic Kelvin-

© 0000 RAS

Helmholtz instability between radially separated co- and counter-rotating thin disc components. Section 3 discusses possible nonlinear consequences of the instability. Section 4 gives the main conclusions.

2 THEORY

2.1 Disc Equilibrium

We consider the stability of a thin counter-rotating disc around a star or black hole. Figure 1 shows the rotation curve we consider. We use an inertial cylindrical (r, ϕ, z) coordinate system. The equilibrium has $(\partial/\partial t = 0)$ and $(\partial/\partial\phi = 0)$, with the flow velocity $\mathbf{u} = u_\phi(r)\hat{\boldsymbol{\phi}} = r\Omega\hat{\boldsymbol{\phi}}$. That is, the accretion velocity u_r and the vertical velocity u_z are assumed negligible compared with u_ϕ. The equilibrium flow satisfies $-\rho r\Omega^2 = -dp/dr + \rho g_r$, where ρ is the density, p the pressure, $g_r = -\partial\Phi/\partial r$ and Φ the gravitational potential. We consider thin discs with half-thickness $h \approx (c_s/u_\phi)r \ll r$, where c_s is the sound speed. In this limit $\Omega = (g_r/r)^{1/2}[1 + \mathcal{O}(h^2/r^2)]$. We consider Keplerian discs where $g_r = GM/r^2$ (with M the mass of the central object) as well as more general discs, for example, flat rotation curve discs relevant to galaxies where $g_r \propto r^{-1}$. We neglect the vertical structure of the equilibrium disc assuming $\partial/\partial z = 0$ for the equilibrium quantities (e.g., ρ, p, and u_ϕ). Our treatment parallels that of Lovelace, Turner, and Romanova (2009; denoted LTR09), but it generalizes that work to include the $z-$dependence of the perturbations.

2.2 Perturbation Equations

The perturbed quantities are: the density, $\tilde{\rho} = \rho + \delta\rho(r, \phi, z, t)$; the pressure is $\tilde{p} = p+\delta p(r, \phi, z, t)$; and the flow velocity is $\tilde{\mathbf{u}} = \mathbf{u} + \delta\mathbf{u}(r, \phi, z, t)$ with $\delta\mathbf{u} = (\delta u_r, \delta u_\phi, \delta u_z)$. We neglect the self-gravity of the disc as commented on at the end of this section. The equations for the perturbed flow are

$$\frac{D\tilde{\rho}}{Dt} + \tilde{\rho}\,\nabla\cdot\tilde{\mathbf{u}} = 0\ , \tag{1}$$

$$\frac{D\tilde{\mathbf{u}}}{Dt} = -\frac{1}{\tilde{\rho}}\nabla\tilde{p} - \nabla\Phi\ , \tag{2}$$

$$\frac{DS}{Dt} = 0\ , \tag{3}$$

where $D/Dt \equiv \partial/\partial t + \tilde{\mathbf{u}}\cdot\nabla$, and where $S \equiv \tilde{p}/(\tilde{\rho})^\gamma$ is the entropy of the disc matter.

We consider perturbations δp, $\delta\rho$.. of the form

$$f(r)\exp(im\phi + ik_z - i\omega t), \tag{4}$$

where $m = 0, 1, 2, ..$ is the azimuthal mode number, ω the angular frequency, and k_z the wavenumber in the $z-$direction. From equation (1), we find

$$i\Delta\omega\ \delta\rho = \nabla\cdot(\rho\ \delta\mathbf{u})\ , \tag{5}$$

where $\Delta\omega(r) \equiv \omega - m\Omega(r)$ and $\Omega = u_\phi/r$. From equation (2),

$$i\Delta\omega\delta u_r + 2\Omega\delta u_\phi = \frac{1}{\rho}\frac{\partial\delta p}{\partial r} - \frac{\delta\rho}{\rho^2}\frac{dp}{dr}\ , \tag{6}$$

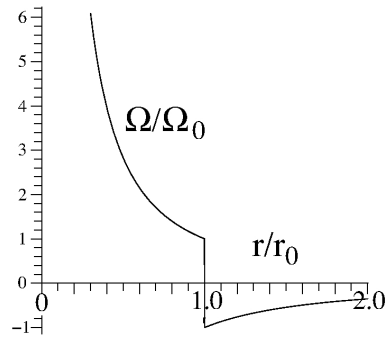

Figure 1. Angular velocity of the counter-rotating Keplerian disc where $g_r = GM/r^2$ with M the mass of the central object.

$$i\Delta\omega\delta u_\phi - \frac{\kappa^2}{2\Omega}\delta u_r = ik_\phi\frac{\delta p}{\rho}\ , \tag{7}$$

$$i\Delta\omega\delta u_z = ik_z\frac{\delta p}{\rho}\ . \tag{8}$$

Here,

$$\kappa \equiv \left[\frac{1}{r^3}\frac{d(r^4\Omega^2)}{dr}\right]^{\frac{1}{2}}$$

is the radial epicyclic frequency and $k_\phi \equiv m/r$ is the azimuthal wavenumber. From equation (3) we have

$$\delta p = c_s^2 - \frac{i\rho c_s^2}{\Delta\omega L_S}\delta u_r\ , \tag{9}$$

where

$$\frac{1}{L_S} \equiv \frac{1}{\gamma}\frac{d\ln(S)}{dr}\ , \qquad c_s \equiv \left(\frac{\gamma p}{\rho}\right)^{1/2}\ , \tag{10}$$

with L_S the length scale of the disc's entropy variation, and c_s the sound speed.

Introducing $\Psi \equiv \delta p/\rho$, equations (6)-(8) can be rewritten as

$$\rho\delta u_r = i\mathcal{F}\left[\frac{\Delta\omega}{\Omega}\left(\frac{\partial\Psi}{\partial r} - \frac{\Psi}{L_*}\right) - 2k_\phi\Psi\right]\ , \tag{11}$$

$$\rho\delta u_\phi = \mathcal{F}\Bigg\{\frac{\kappa^2}{2\Omega^2}\left(\frac{\partial\Psi}{\partial r} - \frac{\Psi}{L_S}\right) - k_\phi\left(\frac{\Delta\omega}{\Omega} + \frac{dp/dr}{\rho\Omega\Delta\omega L_S}\right)\Psi\Bigg\}\ , \tag{12}$$

$$\rho\delta u_z = \rho\frac{k_z}{\Delta\omega}\Psi, \tag{13}$$

where

$$\mathcal{F} \equiv \frac{\rho\Omega}{\mathcal{D}}\ , \tag{14}$$

and

$$\mathcal{D} = \kappa^2 - (\Delta\omega)^2 - \frac{dp/dr}{\rho L_S}\ . \tag{15}$$

Equations (9) and (11) can be combined to give

$$\delta\rho = \frac{\rho\Psi}{c_s^2} - \frac{\mathcal{F}}{\Delta\omega L_S}\left[\frac{\Delta\omega}{\Omega}\left(\frac{\partial\Psi}{\partial r} - \frac{\Psi}{L_S}\right) - 2k_\phi\Psi\right]. \tag{16}$$

Equations (11)-(13) and (16) can now be substituted into equation (5) to give a single differential equation for $\Psi(r)$,

$$\frac{1}{r}\frac{\partial}{\partial r}\left(\frac{r\mathcal{F}}{\Omega}\frac{\partial\Psi}{\partial r}\right) = \left[\frac{\rho}{c_s^2}+\frac{k_\phi^2\mathcal{F}}{\Omega} + \frac{1}{r}\frac{\partial}{\partial r}\left(\frac{r\mathcal{F}}{\Omega L_S}\right)+\frac{\mathcal{F}}{\Omega L_S^2}\right]\Psi + \left[2k_\phi\mathcal{F}\frac{d\ln(g\mathcal{F})}{dr}\right]\frac{\Psi}{\Delta\omega} + \left[\frac{k_\phi^2(dp/dr)\mathcal{F}}{\rho\Omega L_S}-\rho k_z^2\right]\frac{\Psi}{(\Delta\omega)^2}\ , \quad (17)$$

where $g\equiv\exp(2\int dr/L_S)$. This equation generalizes equation (13) of LTR09 by including the $z-$dependence of the perturbations which contributes the last term in this equation.

The condition neglecting the self-gravity is that the Toomre parameter $Q=\kappa c_s/(\pi G\Sigma)$ be larger than about r/h, where h is the disc's half-thickness and $\Sigma=2h\rho$ is its surface mass density (Lovelace & Hohlfeld 2013).

2.3 Specific Model

In order to simplify the analysis we consider barotropic disc matter where $L_S^{-1}\to 0$ so that $g=1$. Further, we consider the counter-rotation curve shown in Figure 1, namely,

$$\Omega=\begin{cases}(g_r/r)^{1/2} & r<r_0\ ,\\ -(g_r/r)^{1/2} & r>r_0\ .\end{cases} \quad (18)$$

We can then solve equation (17) for Ψ_- for $r<r_0$ and Ψ_+ for $r>r_0$ and then match the solutions to the jump-condition across $r=r_0$ which follows from the equation.

We consider solutions of the form

$$\begin{array}{lll}\Psi_- \propto \exp\left[+k_{r-}(r-r_0)\right], & r<r_0\\ \Psi_+ \propto \exp\left[-k_{r+}(r-r_0)\right], & r>r_0\end{array} \quad (19)$$

We assume $|k_{r\pm}|r_0\gg 1$ so that radial variations of the equilibrium quantities can be neglected. In order that the perturbations decay going away from r_0, we must have $\Re(k_{r\pm})>0$, which can be checked a posteriori.

For $r\gtrless r_0$, equation (17) gives the dispersion relations

$$c_s^2(-k_{r\pm}^2+k_\phi^2)=[\kappa^2-(\Delta\omega_\pm)^2]\left[\frac{k_z^2c_s^2}{(\Delta\omega_\pm)^2}-1\right]\ , \quad (20)$$

where $\Delta\omega_\pm\equiv\omega-m\Omega_\pm$. For $k_z=0$, the dispersion relations take the more familiar form $(\Delta\omega_\pm)^2=\kappa^2+c_s^2(-k_{r\pm}^2+k_\phi^2)$.

It is useful to introduce the following dimensionless variables,

$$\overline{k}_z=k_zh,\ \ \overline{k}_\phi=k_\phi h,\ \ \overline{\Omega}=\frac{\Omega}{\Omega_0},\ \ \overline{\kappa}=\frac{\kappa}{\Omega_0},\ \ \overline{\Delta\omega}=\frac{\Delta\omega}{\Omega_0}\ , \quad (21)$$

where $h=c_s/\Omega_0$ and $\Omega_0=\sqrt{g_r(r_0)/r_0}$. Dropping the over-bars gives $k_{r\pm}(\omega)$,

$$k_{r\pm}^2(\omega)=k_\phi^2-[\kappa^2-(\Delta\omega_\pm)^2]\left[\frac{k_z^2}{(\Delta\omega_\pm)^2}-1\right]\ . \quad (22)$$

Multiplying equation (17) by r, integrating over r from $r_0-\epsilon$ to $r_0+\epsilon$, letting $\epsilon\to 0$, and taking into account that $\Psi(r)$ is continuous across r_0 gives

$$\frac{k_{r+}}{\mathcal{D}_+}+\frac{k_{r-}}{\mathcal{D}_-}=\mathcal{R}(\omega)\ , \quad (23)$$

where

$$\mathcal{R}(\omega)=k_\phi\left(\frac{1}{\mathcal{D}_+}+\frac{1}{\mathcal{D}_-}\right)\left(\frac{1}{\Delta\omega_+}+\frac{1}{\Delta\omega_-}\right)\ . \quad (24)$$

The left-hand side of equation (23) is from the left-hand side of equation (17). The right-hand side, $\mathcal{R}$, is from the right-hand term of equation (17) involving $d\mathcal{F}/dr$ which is $d\mathcal{F}/dr=(\mathcal{F}_+-\mathcal{F}_-)\delta(r-r_0)$.

For the assumed thin discs, $\overline{\Omega}=1+\mathcal{O}(h^2/r_0^2)$ for Keplerian discs and other rotation curves. On the other hand,

$$\mathcal{D}_\pm=\begin{cases}1-(\Delta\omega_\pm)^2 & \text{Keplerian}\ ,\\ \kappa^2-(\Delta\omega_\pm)^2 & \text{other rotation curves}\ ,\end{cases} \quad (25)$$

and $\Delta\omega_\pm=\omega\pm m$ with ω measured in units of Ω_0.

Equation (23) can be squared twice to obtain

$$G(\omega)=\left(\frac{k_{r+}^2}{\mathcal{D}_+^2}-\frac{k_{r-}^2}{\mathcal{D}_-^2}-\mathcal{R}^2\right)^2-\frac{4k_{r-}^2\mathcal{R}^2}{\mathcal{D}_-^2}=0\ . \quad (26)$$

The possibility of spurious roots of this equation not satisfying equation (23) has to be checked a posteriori. Equation (26) can be expanded out as a 16th order polynomial in ω.

Important properties of $G(\omega)$ are readily verified: Firstly, for $m=0$ the perturbation is stable, $\mathcal{R}=0$ and therefore $k_{r+}=k_{r-}=0$ so that either $\omega=\pm\kappa$ (radial epicyclic motion) or $\omega=\pm k_z$ (vertically propagating sound wave). For this reason we consider $m\geqslant 1$ in the following. Secondly, $G(\omega)=G(-\omega)$. Thirdly, $[G(\omega)]^*=G(\omega^*)$. It follows that the solutions for ω of $G(\omega)=0=[G(\omega)]^*$ are either purely real or purely imaginary.

The roots of $G(\omega)$ can be located by making a contour plot of

$$F(\omega)=\left\{\Re[G(\omega)]\right\}^2+\left\{\Im[G(\omega)]\right\}^2\ , \quad (27)$$

in the $\omega=\omega_R+i\omega_I$ plane with Maple or Mathematica. Figure 2 shows the the unstable roots for low m values for a Keplerian disc with $h/r_0=0.1$. There is stability ($\omega=$ real) for $k_z<k_{zc}(m)$. For this range of k_z, the ω roots are real. We have verified that for $k_z>k_{zc}$ the roots satisfy equation (23) as well as the conditions $\Re(k_{r\pm})>0$ needed for the modes to be localized around r_0. Figure 3 shows the real and imaginary parts of $k_{r\pm}$ as a function of k_z for $m=1$ also for a Keplerian disc with $h/r_0=0.1$.

A significant simplification of the dispersion relation (26) is possible in the limit where $k_z\gg k_\phi=m(h/r_0)$. In this limit,

$$k_{r\pm}=-\mathcal{D}_\pm\left(\frac{k_z^2}{\Delta\omega_\pm^2}-1\right)\ , \quad (28)$$

and

$$\frac{k_{r+}^2}{\mathcal{D}_+^2}=\frac{k_{r-}^2}{\mathcal{D}_-^2}\ . \quad (29)$$

By combining equations (28) and (29) we obtain a function with roots that can be determined analytically. By rewriting this function as an ordinary polynomial, we obtain a 9-th order polynomial. Factoring out the $\omega=0$ root gives the

8-th order polynomial

$$\omega^8 - (2\kappa^2 + 2k_z^2 + 4m^2)\omega^6 + (\kappa^4 + 5k_z^2\kappa^2 + 2m^2\kappa^2 + 2k_z^2m^2 + 6m^4)\omega^4 + (-4k_z^2\kappa^4 - 2m^2\kappa^4 + 6k_z^2m^2\kappa^2 + 2m^4\kappa^2 + 2k_z^2m^4 - 4m^6)\omega^2 + (k_z^2\kappa^6 - 4k_z^2m^2\kappa^4 + m^4\kappa^4 + 5k_z^2m^4\kappa^2 - 2m^6\kappa^2 - 2k_z^2m^6 + m^8) = 0 \ . \quad (30)$$

Rewriting the equation in this form removes the duplicate solutions from the original polynomial. There are four real roots, $\omega_R = \pm(m \pm \kappa)$ which are the normal modes of a unidirectional disc, and the four roots

$$\omega = \pm\left[k_z^2 + m^2 + \sqrt{k_z^2(-\kappa^2 + k_z^2 + 4m^2)}\right]^{1/2} \ , \quad \omega = \pm\left[k_z^2 + m^2 - \sqrt{k_z^2(-\kappa^2 + k_z^2 + 4m^2)}\right]^{1/2} \ . \quad (31)$$

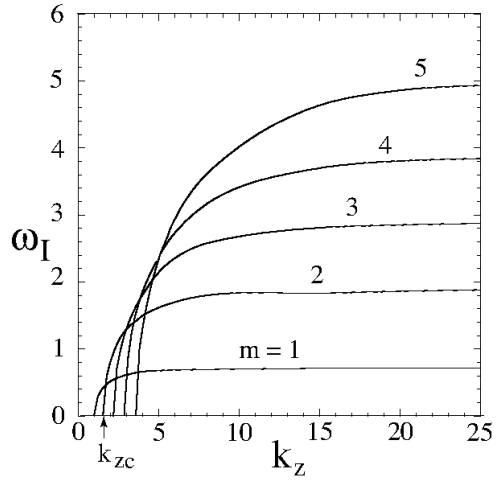

Figure 2. Wavenumber dependence of the growth rate of the instability, $\Im(\omega) = \omega_I$, for different values of m for a Keplerian disc with $h/r_0 = 0.1$. Note that ω_I is in units of Ω_0 and k_z is in units of h^{-1}.

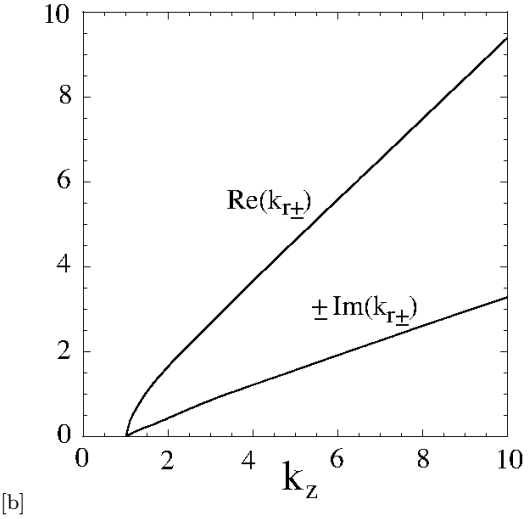

[b]

Figure 3. Radial wavenumber, $\Re(k_{r\pm})$ and $\Im(k_{r\pm})$, as a function of k_z for $m = 1$ for a Keplerian disc with$h/r_0 = 0.1$. The wavenumbers are in units of h^{-1}.

The first set of roots give stable oscillations. The second set gives purely imaginary ω values. The unstable root is

$$\omega_I = \left[\sqrt{k_z^2(k_z^2 + 4m^2 - \kappa^2)} - m^2 - k_z^2\right]^{1/2} \ . \quad (32)$$

For k_z large compared with unity, $\omega_I \to m$.

Solving for $\omega_I = 0$ gives the threshold value

$$k_{zc} = \left[\frac{m^4}{2m^2 - \kappa^2}\right]^{1/2} \ . \quad (33)$$

This expression agrees accurately with the solutions obtained from the full dispersion relation (equation 23). Note that for a Keplerian disc, $\kappa = 1$, so that all of the modes $m = 1, 2, ..$ are unstable. For flat rotation curves relevant to disc galaxies, u_ϕ =const, so that $\kappa = \sqrt{2}$ and consequently

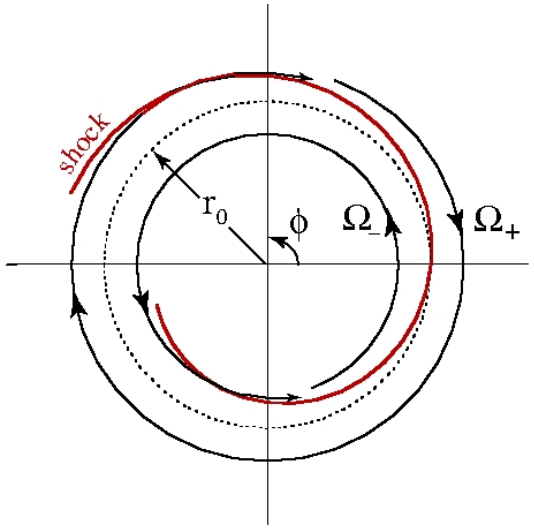

[h]

Figure 4. Polar plot of a one armed ($m = 1$) perturbation which has steepened to form an oblique shock. The gas crossing the shock is deflected towards the interface of the two components.

the mode $m = 1$ is stable. This mode is also stable for a rigid rotation curve disc where $\kappa = 2$. Note that the dependence of the growth rate on κ shows the dependence of the instability on the curvature of the disc.

The growth rates found here are in approximate agreement with the predictions for a planar vortex sheet $\omega^2 = (k_\parallel c_s)^2[1 + \mathcal{M}_p^2/4 - (1 + \mathcal{M}_p^2)^{1/2}]$, where $\mathcal{M}_p \equiv (k_\phi/k_\parallel)\mathcal{M}_T \leqslant \mathcal{M}_T$ with $k_\parallel = \sqrt{k_\phi^2 + k_z^2}$ the wavenumber parallel to the interface, and $\mathcal{M}_T = 2r_0\Omega_0/c_s$ the Mach number of the total velocity jump (see, e.g., Choudhury & Lovelace 1984). In this case, instability $\omega^2 < 0$ occurs for $\mathcal{M}_p < 2^{3/2}$ which corresponds to $k_z h > m(1/2 - h^2/r_0^2)^{1/2} \approx m/\sqrt{2}$. This agrees with equation (33) for $\kappa = 0$. The correspondence of the instability found here and the vortex sheet instability establishes that the instability found here is the supersonic Kelvin-Helmholtz instability. Landau's (1944) study of the stability of a supersonic vortex sheet assumed $k_z = 0$ and found linear stability for $\mathcal{M}_T > 2^{3/2}$. However, under this condition linear instability occurs for $k_z \neq 0$ when $\left[k_\phi(k_\phi^2 + k_z^2)^{-1/2}\right]\mathcal{M}_T < 2^{3/2}$.

3 NONLINEAR EVOLUTION

Although the growth rate increases with increasing wavenumber k_z, the large k_z modes are not expected to be important because their growth will saturate at a small amplitude $\delta r \sim k_z^{-1}$ and involve mixing only small amounts of co- and counter-rotating matter. For this reason we consider the long wavelength modes, $k_z \sim h^{-1}$ and $k_\phi \geqslant r_0^{-1}$. The perturbations have the form

$$\Psi_\pm \propto \exp\left[\mp\Re(k_{r\pm})(r - r_0)\right]\exp\left[i(m\phi \mp \Im(k_{r\pm})(r - r_0)\right]. \quad (34)$$

The maximum of the perturbation is a tightly-wrapped leading spiral $r = r_0 \pm m\phi/\Im(k_{r\pm})$ with m arms. Figure 4 shows the nature of the spiral for $m = 1$.

The spiral wave can lead to the formation of an oblique shock under some conditions. Upstream of the wave, the magnitude of the normal normal component of the gas velocity relative to the wave is $u_n = \theta r_0\Omega_0$, where $\theta = m|\Im(k_{r\pm})r_0|^{-1} \ll 1$. If the upstream normal Mach number $\mathcal{M}_n = u_n/c_s > 1$ there is an oblique shock. On the downstream side the normal Mach number is less than unity. For $r > r_0$ the gas is deflected inward and acquires a radial velocity $u_r = -\beta r_0\Omega_0$, where $\beta = [2/(1 + \gamma)](1 - \mathcal{M}_n^{-2})\theta$. For $r < r_0$, the oblique shock gives outward radial velocity $u_r = \beta r_0\Omega_0$.

The co- and counter-rotating disc components have a natural *repulsion* for each other for the following reason. The mixing of the two components will involve strong shocks. A possible geometry for $m = 1$ is sketched in Figure 5 where there are two strong standing shocks, each with Mach number $\mathcal{M} = u_\phi/c_s \gg 1$. In the region between the shocks, the angular momenta of the two components is annihilated and the gas is strongly heated. The ratio of the gas temperatures downstream to upstream of the normal shock is $T_2/T_1 \approx 1 + 2(\gamma - 1)\gamma\mathcal{M}^2/(\gamma + 1)^2$. This ratio is ~ 20 for $\mathcal{M} = 10$ and $\gamma = 7/5$. The heated gas will expand vertically increasing its scale height by a factor $\sqrt{T_2/T_1} \gg 1$. With no centrifugal force, the gas will free-fall over the surfaces of the inner disc towards the disc's center.

The mass loss rate from this process is $\dot{M}_{\rm ann} = 4mhr_0\Delta r\rho\Omega_0$, where Δr is the radial amplitude of the interface perturbation. This loss rate is larger than the Shakura-Sunyaev (1973) accretion rate by a factor of order $(m/\pi)(\Delta r/h)(\mathcal{M}/\alpha)$ where α is the dimensionless viscosity coefficient for a disc rotating in one direction. It is commonly estimated to be in the range $10^{-3} - 0.1$. The Kelvin-Helmholtz instability evidently gives a spatially localized effective viscosity coefficient $\alpha_{\rm eff} \sim (m/\pi)\mathcal{M}$ assuming $\Delta r \sim h$. Thus the region between the co- and counter-rotating components will be rapidly emptied of gas and a gap will form. Subsequently, the outer disc will spread inward and the inner disc outward due to the turbulent viscosity. Consequently the gap will close after a definite period and the mentioned heating and annihilation of angular momentum will repeat.

4 CONCLUSIONS

Observations of galaxies and models of accreting systems point to the occurrence of counter-rotating discs where the inner part of the disc ($r < r_0$) is co-rotating and the outer part is counter-rotating. This work analyzes the linear stability of radially separated co- and counter-rotating thin discs. The strong instability is the supersonic Kelvin-Helmholtz instability. The growth rates are of the order of or larger than the angular rotation rate at the interface $\Omega(r_0)$. The instability is absent if there is no vertical dependence of the perturbation, that is, if $k_z = 0$. That is, the instability is essentially a three-dimensional instability. Thus this instability is not captured by the analysis of Li and Narayan (2004) where $k_z = 0$ and where the gas is treated as incompressible. Counter-rotating Keplerian discs are unstable for azimuthal mode numbers $m = 1, 2, ..$, whereas for a flat rotation curve relevant to disc galaxies the unstable mode numbers are $m = 2, 3, ...$ We note that when there is a density change across the interface there is necessarily a

corresponding change in the entropy. This changes the jump condition across the interface and leads in general to propagating unstable modes where $\omega = \omega_R + i\omega_I$ with $\omega_R \neq 0$ and $\omega_I > 0$. The important new term in the jump condition comes from the term $(\mathcal{F}/\Omega L_S^2)\Psi$ on the right-hand side of equation (17).

The nonlinear phase of the instability will involve the mixing of co- and counter-rotating gas which will involve strong shocks, strong heating of the gas, and annihilation of the angular momenta of the two gas components. The heated gas will expand vertically and since it has zero angular momentum it will free-fall to the disc's center over the surface of the inner disc. Thus the region between the co- and counter-rotating components will be rapidly emptied of gas and a gap will form. In effect the two components have a repulsive interaction. This is suggestive of the Leidenfrost effect (Leidenfrost 1966) where a liquid droplet is levitated above a hot surface by the vapor pressure between the droplet and the surface. Subsequent to the gap formation, the outer disc will spread inward and the inner disc outward due to the turbulent viscosity. Consequently the gap will close after a definite period and the heating and annihilation of angular momentum will repeat.

Three-dimensional hydrodynamic simulations are of course required to fully understand the nonlinear evolution of the counter-rotating discs. Although axisymmetric disc simulations do not allow for the Kelvin-Helmholtz instability, the inclusion of viscosity can model the effect of the turbulent viscosity due to the instability. In an early study by Kuznetsov et al. (1999) the effective viscosity was the numerical viscosity due to the finite grid. In a recent study by Dyda et al. (2014), a high resolution grid was used with all components of the viscous stress tensor are included to model an isotropic Shakura-Sunyaev $\alpha-$viscosity. Both studies clearly show the development of a gap between the co- and counter-rotating components and enhanced accretion. The study by Dyda et al. (2014) shows the quasi periodic closing and opening of the gap.

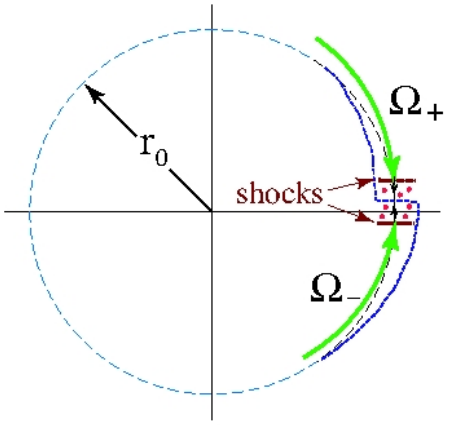

Figure 5. Polar plot suggesting the formation of strong normal shocks leading the annihilation of the angular momenta of the co- and counter rotating components and the heating of this gas.

ACKNOWLEDGMENTS

We thank M.M. Romanova for valuable discussions and an anonymous referee for valuable comments. This work was supported in part by NASA grants NNX11AF33G and NSF grant AST-1211318.

REFERENCES

Braun, R., Walterbos, R.A.M., Kennicutt, R.C., & Tacconi, L.J. 1994, ApJ, 420, 558
Chakrabarty, D., Bildsten, L., Finger, M. H., Grunsfeld, J. M., Koh, D. T., Nelson, R. W., Prince, T. A., Vaughan, B. A., & Wilson, R. B. 1997, ApJ, 481, L101
Choudhury, S.,R., & Lovelace, R.V.E, 1984, ApJ, 283, 331
Corsini, E.M. 2014, in *Counter-Rotation in Disk Galaxies*, ASP Conference Series, Vol. 486, Eds. E. Iodice & E. M. Corsini (ASP: San Francisco), p. 51
Dyda, S., Lovelace, R.V.E., Ustyugova, G.V., Romanova, M.M., & Koldoba, A.V. 2014, MNRAS. submitted
Galetta, G. 1996, in *Barred Galaxies*, IAU Colloq. 157, Eds. R. Buta, D. Crocker, & B. Elmegreen, ASP Conference Series, 91, 11
King, A.R., & Pringle, J.E. 2006, MNRAS, 373, L90
King, A.R., & Pringle, J.E. 2007, MNRAS, 377, L25
Kuznetsov, O. A., Lovelace, R. V. E., Romanova, M. M., & Chechetkin, V. M. 1999, ApJ, 514, 691
Landau, L. 1944, Dokl. Akad. Nauk SSSR, V. XLIV, 339
Leidenfrost, J.G. 1966, Int. J. Heat Mass Transfer, 9, 1153

Li, L., & Narayan, R., 2004, ApJ, 601, 414
Lovelace, R.V.E., & Chou, T., 1996, ApJ, 468, L25
Lovelace, R.V.E., Turner, L., & Romanova, M.M. 2009, ApJ, 701, 225
Lovelace, R.V.E. & Hohlfeld, R.G. 2013, MNRAS, 429, 529
Nelson, R. W., Bildsten, L., Chakrabarty, D., Finger, M. H., Koh, D. T., Prince, T.A., Rubin, B. C., Scott, D. M., Vaughan, B. A., & Wilson, R, B. 1997, ApJ, 488, L117
Nixon, C.J., King, A.R., & Price, D.J. 2012, MNRAS, 422, 2547
Remijan, A.J., & Hollis, J.M. 2006, ApJ, 640, 842
Rubin, V.C. 1994a, AJ, 107, 173
Rubin, V.C. 1994b, AJ, 108, 456
Shakura, N.I., & Sunyaev, R.A. 1973, A&A, 24, 337
Tang, Y.W., Guilloteau, S., Piétu, V., Dutrey, A., Ohashi, N., & Ho, P.T.P., 2012, A&A, 547, A84